Here, J is the Jacobian matrix, presented by Equation (22) and evaluated at the steady state. It is clear from Equation (A2) that the derivatives of the outlet conditions are given by

$$\begin{bmatrix} d\gamma_e/d\theta_F \\ \\ d\theta_e/d\theta_F \end{bmatrix} = (J-I)^{-1} J \begin{bmatrix} 0 \\ \\ 1-1/R_r \end{bmatrix} \qquad (A3)$$

The inverse of the matrix $(J-I)$, which exists whenever its determinant does not vanish, may be expressed as

$$(J-I)^{-1} = \frac{1}{d-tr+1} \begin{bmatrix} R_r\,\partial\theta_e/\partial\theta_o - 1 & -R_r\,\partial\gamma_e/\partial\theta_o \\ -R_r\left[\partial\theta_e/\partial\gamma_o + \sum_{i=1}^{m-1} \partial\theta_e/\partial\gamma_{io}\right] & R_r\left[\partial\gamma_e/\partial\gamma_o + \sum_{i=1}^{m-1} \partial\gamma_e/\partial\gamma_{io}\right] - 1 \end{bmatrix} \qquad (A4)$$

The following expression for $d\gamma_e/d\theta_F$ can be readily obtained from Equations (A3) and (A4).

$$d\gamma_e/d\theta_F = \frac{1-R_r}{d-tr+1}\,\partial\gamma_e/\partial\theta_o \qquad (A5)$$

Since the characteristic equation, as given in Equation (42), of the Jacobian matrix J can be written in the form

$$\lambda^2 - tr\,\lambda + d = 0 \qquad (A6)$$

it can readily be shown that whenever the quantity $(d - tr + 1)$ in Equation (A5) is negative, one of the solutions of Equation (A6) exceeds unity. Consequently, the corresponding steady state is unstable. It follows that a necessary, but not sufficient, condition for steady state stability is that the sign of $d\gamma_e/d\theta_F$ be the same as the sign of $\partial\gamma_e/\partial\theta_o$.

This condition can now be applied to show that the intermediate conversion state is always unstable for irreversible reactions such as those considered in the preceding examples. An examination of the curves in Figure 4 shows that $d\gamma_e/d\theta_F$ never vanishes; thus it follows from Equation (A5) that the sign of $\partial\gamma_e/\partial\theta_o$ can never change. Furthermore, the sign of $\partial\gamma_e/\partial\theta_o$ must be negative, since one can argue that, at least at sufficiently low inlet temperatures, the outlet reactant concentration would be expected to decrease with an increase in inlet temperature for an irreversible reaction. An intermediate conversion steady state violates the above condition for stability, therefore, since $d\gamma_e/d\theta_F$, being positive, does not agree in sign with $\partial\gamma_e/\partial\theta_o$.

Manuscript received August 19, 1965; revision received November 11, 1965; paper accepted November 15, 1965.

The Finite-Difference Computation of Natural Convection in a Rectangular Enclosure

J. O. WILKES and S. W. CHURCHILL

University of Michigan, Ann Arbor, Michigan

A study is made of the natural convection of a fluid contained in a long horizontal enclosure of rectangular cross section with one vertical wall heated and the other cooled. Two-dimensional motion is assumed. The governing vorticity and energy transport equations are solved by an implicit alternating direction finite-difference method. Transient and steady state isothermals and streamlines are obtained for Grashof numbers up to 100,000 and for height-to-width ratios of 1, 2, and 3.

This work is part of a research program whose object is to develop numerical methods for solving the partial differential equations governing the conservation of mass, momentum, and energy in problems of natural and free convection. In the initial investigation (7), Martini and Churchill measured the temperature and velocity fields for air contained in a long hollow horizontal cylinder with one vertical half heated and the other cooled. They did not complete a numerical solution, mainly because of the limitations of the then available computer (an IBM 650). Aided by an IBM 704 computer, Hellums and Churchill (4) developed an explicit finite-difference method for generating the transient solution to the above problem and also for free convection at a vertical plate. In both cases they were able to employ boundary-layer types of equations in which only one momentum balance actually proved to be necessary. The computed transient velocity and temperature fields ultimately converged to steady state values. For the plate, these values agreed excellently with the theoretical solutions of Ostrach (9) and Schmidt

and Beckmann (*12*) and also with the experimental results of the latter. The values computed for the cylinder agreed tolerably well with Martini and Churchill's experimental results.

The object of the present investigation is to extend the finite-difference method to the computation of natural convection in situations in which momentum transfer is significant in two dimensions. The motion of a fluid in a long horizontal enclosure of rectangular cross section with one vertical side heated and the other cooled is chosen for study. For purposes of simplifying the problem, two-dimensional motion is assumed; the possibility of computing a completely turbulent solution is thereby precluded. For moderately low Rayleigh numbers, Poots' analytical steady state solution is available (*11*) for checking the computed values. Poots expressed temperature and stream function as two doubly infinite series of orthogonal functions, and presented numerical values for a square cross section with a linear variation of temperature along the top and bottom horizontal walls for $500 < N_{Ra} < 10{,}000$.

Batchelor (*1*) also investigated the following special cases for natural convection in a rectangular cavity: small N_{Ra} ($< 10^3$) with L approximately unity, large L for general N_{Ra}, and large N_{Ra} for general L; he was forced to make drastic idealizations to obtain solutions for the last two cases. He predicted transition to turbulent flow at $N_{Gr} = 13{,}700$ for the second case and at $N_{Ra}L^3 = 10^9$ for the third case. Eckert and Carlson (*2*) observed the temperature distribution interferometrically and derived the heat transfer rate for several conditions. Mull and Reiher (*8*) also measured the heat transfer rate across enclosed horizontal, oblique, and vertical air layers. Batchelor's predictions were between 50 and 100% higher than these measurements.

PROBLEM STATEMENT

The physical situation is illustrated in Figure 1. The fluid is initially motionless and at a uniform temperature equal to the average of the vertical wall temperatures. Two alternative boundary conditions are considered for temperature on the horizontal walls, namely perfect insulation, and a linear variation $\theta = \theta_1 + (\theta_2 - \theta_1)y/d$. The problem is to find the subsequent velocities and temperatures as functions of time and position and the rate of heat transfer across the enclosure as a function of time. A final steady state solution, if such exists, would be of particular interest.

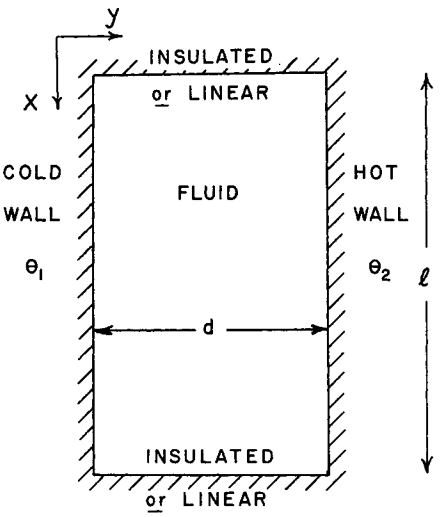

Fig. 1. Rectangular enclosure.

The appropriate equations of motion and continuity are (*13*)

$$\frac{\partial u}{\partial t} + u\frac{\partial u}{\partial x} + v\frac{\partial u}{\partial y} = -g\beta(\theta - \theta_0) - \frac{1}{\rho}\frac{\partial p'}{\partial x} + \nu\left(\frac{\partial^2 u}{\partial x^2} + \frac{\partial^2 u}{\partial y^2}\right) \tag{1}$$

$$\frac{\partial v}{\partial t} + u\frac{\partial v}{\partial x} + v\frac{\partial v}{\partial y} = -\frac{1}{\rho}\frac{\partial p'}{\partial y} + \nu\left(\frac{\partial^2 v}{\partial x^2} + \frac{\partial^2 v}{\partial y^2}\right) \tag{2}$$

$$\frac{\partial u}{\partial x} + \frac{\partial v}{\partial y} = 0 \tag{3}$$

In deriving these equations, one treats the fluid properties as constants, except for one step in which a temperature variation of density is essential to the phenomenon of natural convection. The additional assumption is made that the applied temperature difference $(\theta_2 - \theta_1)$ is small compared with $1/\beta$.

If viscous dissipation and compressibility effects are neglected, the corresponding energy balance is

$$\frac{\partial \theta}{\partial t} + u\frac{\partial \theta}{\partial x} + v\frac{\partial \theta}{\partial y} = \frac{k}{\rho c_p}\left(\frac{\partial^2 \theta}{\partial x^2} + \frac{\partial^2 \theta}{\partial y^2}\right) \tag{4}$$

The initial and boundary conditions are

$$\left.\begin{array}{l} t = 0,\ 0 \le x \le l,\ 0 \le y \le d\text{: } u = v = 0,\ \theta = \theta_0, \\ x = 0 \text{ and } x = l\text{: } u = v = 0,\ \theta = \theta_1 + (\theta_2 - \theta_1)y/d \\ \qquad\qquad \text{or } \partial\theta/\partial x = 0, \\ y = 0\text{: } u = v = 0,\ \theta = \theta_1, \\ y = d\text{: } u = v = 0,\ \theta = \theta_2 \end{array}\right\} \quad t > 0 \tag{5}$$

The above equations may be restated in the following dimensionless forms:

$$\frac{\partial U}{\partial \tau} + U\frac{\partial U}{\partial X} + V\frac{\partial U}{\partial Y} = -\frac{N_{Gr}\,T}{2} - \frac{\partial P}{\partial X} + \frac{\partial^2 U}{\partial X^2} + \frac{\partial^2 U}{\partial Y^2} \tag{6}$$

$$\frac{\partial V}{\partial \tau} + U\frac{\partial V}{\partial X} + V\frac{\partial V}{\partial Y} = -\frac{\partial P}{\partial Y} + \frac{\partial^2 V}{\partial X^2} + \frac{\partial^2 V}{\partial Y^2} \tag{7}$$

$$\frac{\partial T}{\partial \tau} + U\frac{\partial T}{\partial X} + V\frac{\partial T}{\partial Y} = \frac{1}{N_{Pr}}\left(\frac{\partial^2 T}{\partial X^2} + \frac{\partial^2 T}{\partial Y^2}\right) \tag{8}$$

$$\frac{\partial U}{\partial X} + \frac{\partial V}{\partial Y} = 0 \tag{9}$$

$$\left.\begin{array}{l} \tau = 0,\ 0 \le X \le L,\ 0 \le Y \le 1\text{: } U = V = 0,\ T = 0 \\ X = 0 \text{ and } X = L\text{: } U = V = 0,\ T = 2Y - 1 \\ \qquad\qquad \text{or } \partial T/\partial X = 0, \\ Y = 0\text{: } U = V = 0,\ T = -1, \\ Y = 1\text{: } U = V = 0,\ T = 1 \end{array}\right\} \quad \tau > 0 \tag{10}$$

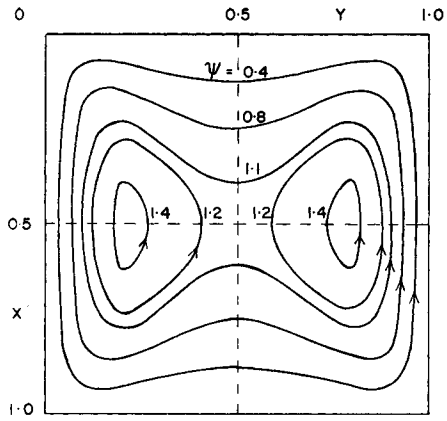

Fig. 2. Transient streamlines ($\tau = 0.004$).

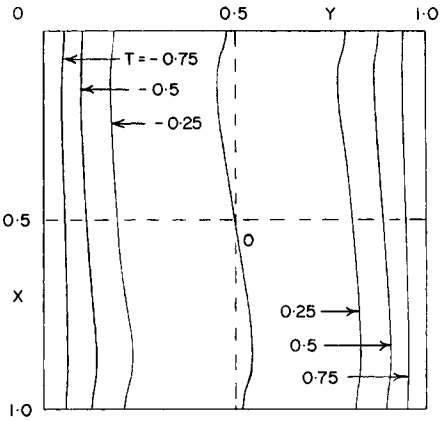

Fig. 3. Transient isothermals ($\tau = 0.01$).

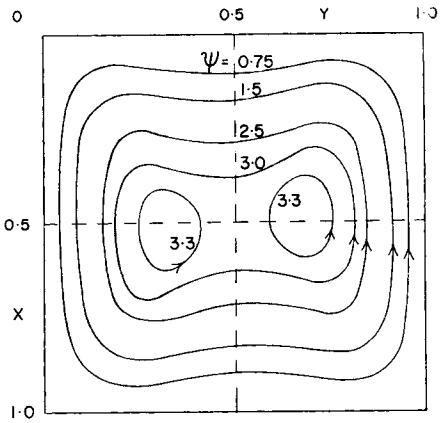

Fig. 4. Transient streamlines ($\tau = 0.01$).

Differentiating Equations (6) and (7) with respect to Y and X, respectively, subtracting, and applying Equation (9) produces the following equation in which pressure no longer appears:

$$\frac{\partial}{\partial \tau}\left(\frac{\partial U}{\partial Y} - \frac{\partial V}{\partial X}\right) + U\frac{\partial^2 U}{\partial X \partial Y} + V\frac{\partial^2 U}{\partial Y^2} - U\frac{\partial^2 V}{\partial X^2}$$

$$- V\frac{\partial V^2}{\partial X \partial Y} = -\frac{N_{Gr}}{2}\frac{\partial T}{\partial Y} + \frac{\partial(\nabla^2 U)}{\partial Y} - \frac{\partial(\nabla^2 V)}{\partial X} \quad (11)$$

The introduction of a dimensionless vorticity $\zeta = -\nabla^2\psi$, where the dimensionless stream function ψ is such that $U = \partial\psi/\partial Y$ and $V = -\partial\psi/\partial X$, enables the problem statement to be written as

$$\frac{\partial \zeta}{\partial \tau} + U\frac{\partial \zeta}{\partial X} + V\frac{\partial \zeta}{\partial Y} = \frac{N_{Gr}}{2}\frac{\partial T}{\partial Y} + \nabla^2\zeta \quad (12)$$

$$\frac{\partial T}{\partial \tau} + U\frac{\partial T}{\partial X} + V\frac{\partial T}{\partial Y} = \frac{1}{N_{Pr}}\nabla^2 T \quad (13)$$

$$\nabla^2\psi = -\zeta \quad (14)$$

$$U = \frac{\partial \psi}{\partial Y}, \quad V = -\frac{\partial \psi}{\partial X} \quad (15)$$

$$\left.\begin{array}{l} \tau = 0,\ 0 \leq X \leq L,\ 0 \leq Y \leq 1\text{: } \zeta = 0,\ T = 0, \\ X = 0 \text{ and } X = L\text{: } \psi = \partial\psi/\partial X = 0, \\ \qquad T = 2Y - 1 \text{ or } \partial T/\partial X = 0 \\ Y = 0\text{: } \psi = \partial\psi/\partial Y = 0,\ T = -1, \\ Y = 1\text{: } \psi = \partial\psi/\partial Y = 0,\ T = 1. \end{array}\right\} \quad \tau > 0 \quad (16)$$

TABLE 1. OPTIMUM VALUES OF RELAXATION PARAMETER FOR USE IN EQUATION (19)

No. of grid spacings: X direction	Y direction	$\Delta X\ (= \Delta Y)$	ω_{opt}
10	10	0.2	1.58
20	20	0.05	1.83
20	10	0.1	1.70
30	10	0.1	1.73

The velocities U and V are retained explicitly in the problem formulation, since their computed values will give an immediate picture of the flow pattern. The local Nusselt number is $N_{Nu} = (\partial T/\partial Y)_{Y=0}/2$, and its mean value $N_{\overline{Nu}}$ over the height of the enclosure will depend on N_{Gr}, N_{Pr}, L, and τ. For conduction alone, N_{Nu} and $N_{\overline{Nu}}$ would equal unity.

FINITE-DIFFERENCE APPROXIMATION

Equations (12) through (15) here are called the vorticity, temperature, stream function, and velocity equations, respectively. An approximation to their solution will be obtained at a finite number of grid points having coordinates $X = i\Delta X$, $Y = j\Delta Y$, and at discrete times $\tau = n\Delta\tau$, where i, j, and n are integers. The vorticity and temperature equations are parabolic, while the stream function equation is elliptic.

Suppose that all quantities are known at a time $n\Delta\tau$ (the initial condition corresponds to the special case $n = 0$). An implicit alternating direction technique based on suitable finite-difference approximations of the vorticity and temperature equations is employed to advance the fields of vorticity and temperature at the interior grid points across a time step $\Delta\tau$ to the new level $(n + 1)\Delta\tau$. At any grid point the term $\partial T/\partial Y$ in the vorticity equation and the coefficient velocities U and V are treated as constants over a time step. All space derivatives are given centered difference representations.

Thus, the relevant finite-difference approximations to the vorticity equation, to be used consecutively over two half time steps, each of duration $\Delta\tau/2$, are

$$\frac{\zeta^*_{i,j} - \zeta_{i,j,n}}{\Delta\tau/2} + U_{i,j,n}\frac{\zeta^*_{i+1,j} - \zeta^*_{i-1,j}}{2\Delta X} +$$

$$V_{i,j,n}\frac{\zeta_{i,j+1,n} - \zeta_{i,j-1,n}}{2\Delta Y} = \frac{N_{Gr}}{2}\frac{T_{i,j+1,n+1} - T_{i,j-1,n+1}}{2\Delta Y} +$$

$$\delta_X^2\,\zeta^*_{i,j} + \delta_Y^2\,\zeta_{i,j,n} \quad (17)$$

followed by

$$\frac{\zeta_{i,j,n+1} - \zeta^*_{i,j}}{\Delta\tau/2} + U_{i,j,n}\frac{\zeta^*_{i+1,j} - \zeta^*_{i-1,j}}{2\Delta X} +$$

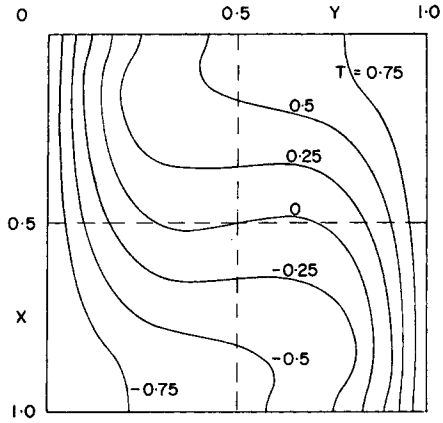

Fig. 5. Steady state isothermals.

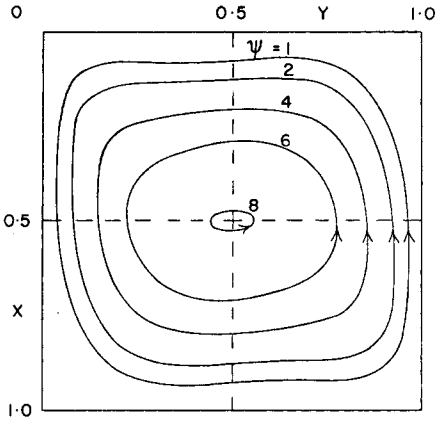

Fig. 6. Steady state streamlines.

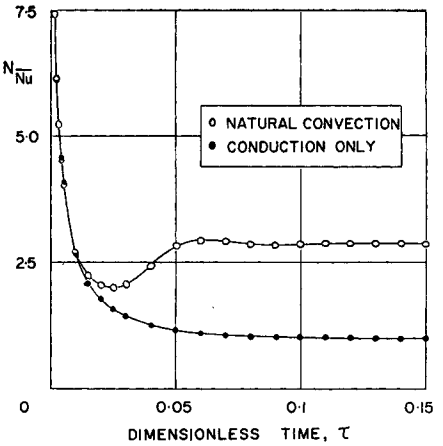

Fig. 7. Mean Nusselt number vs. time.

$$V_{i,j,n}\frac{\zeta_{i,j+1,n+1}-\zeta_{i,j-1,n+1}}{2\Delta Y}=\frac{N_{Gr}}{2}\frac{T_{i,j+1,n+1}-T_{i,j-1,n+1}}{2\Delta Y}+$$

$$\delta_X^2\zeta^*_{i,j}+\delta_Y^2\zeta_{i,j,n+1} \qquad (18)$$

Equations (17) and (18) are implicit in the X and Y directions, respectively, and when applied to every point in a column or row, as the case may be, yield tridiagonal systems in the unknown vorticities $\zeta^*_{i,j}$ or $\zeta_{i,j,n+1}$. Similar approximations also hold for the temperature equation which, in the present calculations, precedes the vorticity equation across a time step.

The method of successive over-relaxation is then employed in conjunction with the newly computed vorticities $\zeta_{i,j,n+1}$ to solve the stream function equation for the new stream function field. Thus, if $\psi^{(m)}_{i,j}$ denotes the approximation at the m^{th} iteration to the stream function at a point, a further approximation $\psi^{(m+1)}_{i,j}$ is obtained from

$$\psi^{(m+1)}_{i,j}=\psi^{(m)}_{i,j}+\frac{\omega}{4}\left[(\Delta X)^2\zeta_{i,j,n+1}+\right.$$

$$\left.\psi^{(m)}_{i-1,j}+\psi^{(m)}_{i+1,j}+\psi^{(m)}_{i,j-1}+\psi^{(m)}_{i,j+1}-4\psi^{(m)}_{i,j}\right] \qquad (19)$$

Once the optimum value ω_{opt} of the relaxation parameter ω has been found by trial and error for a given system of grid points, this value is then employed in all further computations with that grid. Representative values of ω_{opt} for use in Equation (19) are given in Table 1 for various grid systems, each having $\Delta X = \Delta Y$. About twenty-five iterations, with the use of Equation (19) at each grid point, give good convergence.

The new wall vorticities are then computed by considering Taylor's series expansions for stream function in the vicinity of the walls. For example, for points $(i, 1)$ and $(i, 2)$, removed by one and two grid spacings, respectively, in the Y direction from a grid point $(i, 0)$ on the left-hand wall $Y = 0$

$$\psi_{i,1}=\psi_{i,0}+\Delta Y\frac{\partial\psi}{\partial Y}+\frac{(\Delta Y)^2}{2!}\frac{\partial^2\psi}{\partial Y^2}+\frac{(\Delta Y)^3}{3!}\frac{\partial^3\psi}{\partial Y^3} \qquad (20)$$

$$\psi_{i,2}=\psi_{i,0}+2\Delta Y\frac{\partial\psi}{\partial Y}+\frac{(2\Delta Y)^2}{2!}\frac{\partial^2\psi}{\partial Y^2}+\frac{(2\Delta Y)^3}{3!}\frac{\partial^3\psi}{\partial Y^3} \qquad (21)$$

In Equations (20) and (21) all derivatives are considered at the wall point $(i, 0)$. But, from the boundary conditions of Equation (16), both $\psi_{i,0}$ and $\partial\psi/\partial Y$ are zero. After eliminating $\partial^3\psi/\partial Y^3$ between Equations (20) and (21) and noting from the defining equation for vorticity that $\zeta = -\partial^2\psi/\partial Y^2$, the following approximation is obtained for vorticity at the wall:

$$\zeta_{i,0\,n+1}=-\frac{8\psi_{i,1}-\psi_{i,2}}{2(\Delta Y)^2} \qquad (22)$$

That is, the new wall vorticities are computed from stream functions which themselves have been calculated from the new vorticities at the interior grid points. Note that a simpler but less accurate approximation, namely $\zeta_{i,0} = -2\psi_{i,1}/(\Delta Y)^2$, could have been obtained from Equation (20) alone.

Finally, the new fields of U and V are obtained from space centered finite-difference approximations of the velocity equations. The whole process described above is then repeated for as many successive time steps as desired. Further details of the method are given in reference *13*; the successive over-relaxation and implicit alternating direction procedures are also discussed in references 3 and *10*.

RESULTS

Table 2 summarizes the range of the investigations. With the use of a 10 × 10 grid, a typical computation takes less than 3 sec. of IBM 7090 time per time increment. For all runs, the computed values essentially converge to a steady state by a time $\tau = 0.2$. Although not shown here, the steady state temperatures and stream functions of run 4 (20 × 20 grid) are remarkably close to those of run 3 (10 × 10 grid). The 15% difference in $N_{\overline{Nu}}$ between the two is rather an expression of the inherent difficulty in estimating $(\partial T/\partial Y)_{Y=0}$ from values of temperature at grid points extending on one side of the wall only.

To expedite plotting the results, an auxiliary program is written to locate points lying on specified isothermals and streamlines by linear interpolation of the computed values at the grid points. Typical sets of the resulting streamlines and isothermals are shown in Figures 2 through 6 for the conditions of run 3. The value of the stream function at a point is proportional to the flow per unit time crossing any line joining the point to the wall. Thus, the general increase in stream function as time advances shows that the fluid is accelerating. Two anticlockwise eddies develop at first but eventually merge into a single circulation. For small times, the isothermals are roughly parallel

to one another, due to the predominance of conduction. Their later distortion clearly shows the effect of convective energy transport. The stream function at the center of the enclosure actually passes through a maximum before decelerating slightly to its final steady value.

The corresponding variation of heat transfer across the enclosure is shown in Figure 7, again for the conditions of run 3. The finite-difference solution for conduction only is also shown for comparison. The contribution of convection becomes apparent only after $\tau = 0.015$, even though the velocities are by this time well on their way to their final steady values. This is due to the lapse of time occurring while fluid travels from the hot wall to the cold wall, and vice versa. The later "overshoot" (at $\tau = 0.06$) and an even smaller "undershoot" (at $\tau = 0.09$) can be explained similarly.

The transient results for the remaining runs exhibit similar characteristics and are not reproduced here. The steady state results for run 2 (linear type of boundary condition) are also similar, except that the velocities are about 25% higher than those of run 3 (insulated type of boundary condition). The steady state values for run 1 agree almost perfectly with those computed from Poots' solution. The steady state values for the tall rectangle of run 9 are reproduced in Figures 8 and 9. The last column of Table 2 also shows the values of $N_{\overline{Nu}}$ predicted by the following correlation of Jakob (*5, 6*), based on the experiments of Mull and Reiher (*8*):

$$N_{\overline{Nu}} = 0.18\, N_{Gr}^{0.25}\, L^{-0.111},\quad 2 \times 10^4 < N_{Gr} < 2 \times 10^5 \tag{23}$$

For most cases, the computed $N_{\overline{Nu}}$ is from 0 to 70% in excess of that predicted by Equation (23). The discrepancy is due partly to the fact that Jakob's correlation is based on values of L between 3.12 and 42.2, considerably beyond the range investigated here. Indeed, Equation (23) predicts that $N_{\overline{Nu}}$ decreases as L increases, which is unlikely to be true for small values of L.

As shown by runs 3, 5, and 6, $N_{\overline{Nu}}$ for the insulated case depends more strongly on N_{Gr} than predicted by Equation (23), although no simple power law is obeyed. The variation with L is indefinite, since the spread between the $N_{\overline{Nu}}$ of runs 3, 8, and 9 is within the uncertainty of estimating the temperature gradient at the wall. $N_{\overline{Nu}}$ falls appreciably between runs 3 and 7 as the Prandtl number is lowered.

The present technique produces unstable results for Grashof numbers greater than 200,000. This probably arises from the fact that the implicit computation of the *new* interior vorticities supposes that the *old* boundary vorticities still hold good at the end of the time increment. The boundary vorticities themselves are eventually advanced on the basis of Taylor's series expansions for stream function at one and two points removed from the boundary. The resulting slight inconsistency between the in-

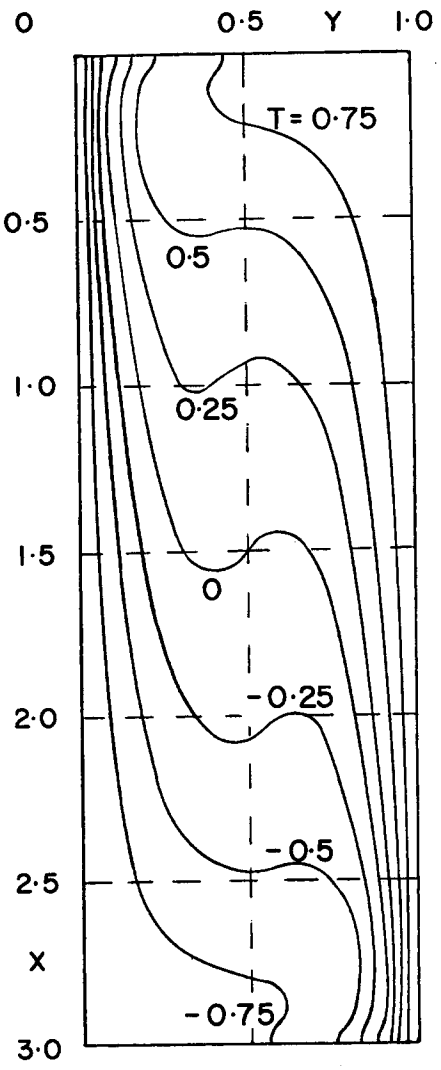

Fig. 8. Steady state isothermals.

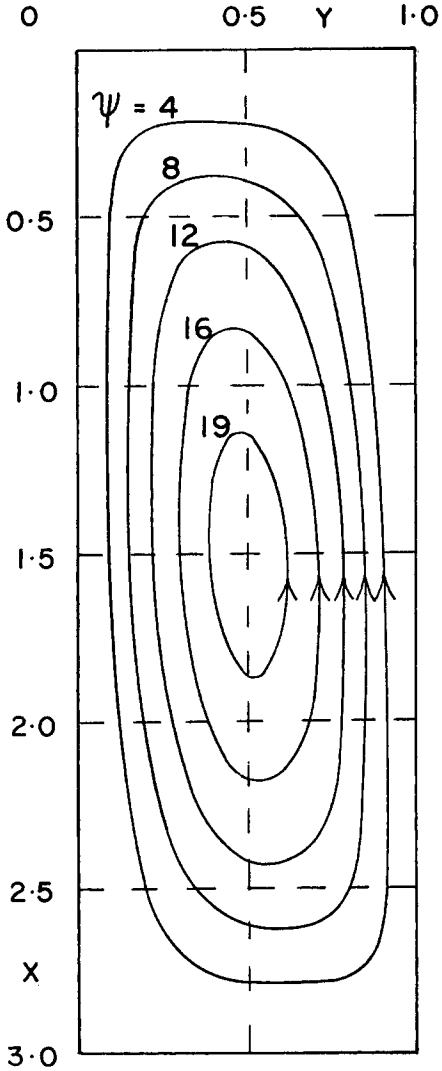

Fig. 9. Steady state streamlines.

TABLE 2. A SUMMARY OF THE COMPUTER RUNS: STEADY STATE MEAN NUSSELT NUMBERS

Run	$\Delta\tau$	L	ΔX	ΔY	N_{Pr}	N_{Gr}	Boundary condition	$N_{\overline{Nu}}$	$N_{\overline{Nu}}$ from Equation (23)
1	0.002	1.0	0.1	0.1	0.733	6,850	Linear	1.419	1.64
2	0.001 and 0.002	1.0	0.1	0.1	0.733	20,000	Linear	2.068	2.14
3	0.001 and 0.002	1.0	0.1	0.1	0.733	20,000	Insulated	2.874	2.14
4	0.001	1.0	0.05	0.05	0.733	20,000	Insulated	2.516	2.14
5	0.001	1.0	0.1	0.1	0.733	60,000	Insulated	4.793	2.82
6	0.001	1.0	0.1	0.1	0.733	100,000	Insulated	5.512	3.20
7	0.002	1.0	0.1	0.1	0.1	20,000	Insulated	1.286	2.14
8	0.002	2.0	0.1	0.1	0.733	20,000	Insulated	2.992	1.98
9	0.002	3.0	0.1	0.1	0.733	20,000	Insulated	2.825	1.89

For heat transfer by conduction only: 1.000

terior and boundary vorticities could be overcome at the expense of iterating several times over each time step.

CONCLUSION

A finite-difference technique has been developed for predicting the transient and steady state natural convection in a rectangular enclosure. The steady state results are in excellent agreement with an existing analytical solution and are not out of line with experiments made under rather different conditions. The paper thus demonstrates the power of numerical methods for the a priori solution of complex problems in convection.

NOTATION

c_p = specific heat
d = width of enclosure
N_{Gr} = Grashof number, $= g\beta(\theta_2 - \theta_1)d^3/\nu^2$
g = acceleration due to gravity
h = local heat transfer coefficient, $= -q/(\theta_2 - \theta_1)$
k = thermal conductivity
l = height of enclosure
L = ratio of cavity height to its width, $= l/d$
N_{Nu} = local Nusselt number, $= hd/k$
$N_{\overline{Nu}}$ = mean value of Nusselt number
p' = pressure deviation from initial (static) value
P = dimensionless pressure deviation, $= p'd^2/\rho\nu^2$
N_{Pr} = Prandtl number, $= \mu c_p/k$
q = heat flux density at a vertical wall
N_{Ra} = Rayleigh number, $= N_{Gr} \times N_{Pr}$
t = time
T = dimensionless temperature, $= (\theta - \theta_0)/(\theta_2 - \theta_0)$
u = velocity in the x direction
U = dimensionless velocity in the X direction, $= ud/\nu$
v = velocity in the y direction
V = dimensionless velocity in the Y direction, $= vd/\nu$
x = vertical coordinate, measured downward from the top left-hand corner of the enclosure
X = dimensionless vertical coordinate, $= x/d$
y = horizontal coordinate, measured across from the top left-hand corner of the enclosure
Y = dimensionless horizontal coordinate, $= y/d$

Greek Letters

ΔX = grid spacing in the X direction
ΔY = grid spacing in the Y direction
$\Delta\tau$ = time increment
∇^2 = Laplacian operator, $= \partial^2/\partial X^2 + \partial^2/\partial Y^2$
ζ = dimensionless vorticity, $= -\nabla^2\psi$
θ = temperature (θ_0, θ_1, and θ_2 refer to the initial temperature, and the temperatures at the cold and hot walls, respectively)
ν = kinematic viscosity
μ = viscosity
ρ = density
τ = dimensionless time, $= t\nu/d^2$
ψ = dimensionless stream function, such that $U = \partial\psi/\partial Y$ and $V = -\partial\psi/\partial X$
β = volume coefficient of thermal expansion
ω = relaxation parameter
δ_X = central difference operator, such that, for example, $\delta_x^2\,\zeta_{i,j,n} = (\zeta_{i-1,j,n} - 2\zeta_{i,j,n} + \zeta_{i+1,j,n})/(\Delta X)^2$

Subscripts

i, j = space subscripts of grid point in X and Y directions
n = time subscript
opt = value of relaxation parameter giving fastest convergence

Superscripts

$*$ = value at the end of a half time step
m = iteration number

LITERATURE CITED

1. Batchelor, G. K., *Quart. Appl. Math.*, **12**, 209-233 (1954).
2. Eckert, E. R. G., and W. O. Carlson, *Intern. J. Heat Mass Transfer*, **2**, 106-120 (1961).
3. Forsythe, G. E., and W. R. Wasow, "Finite Difference Methods for Partial Differential Equations," Wiley, New York (1960).
4. Hellums, J. D., and S. W. Churchill, *A.I.Ch.E. J.*, **8**, 690-695 (1962).
5. Jakob, Max, "Heat Transfer," Vol. I, Wiley, New York (1949).
6. ———, *Trans. Am. Soc. Mech. Engrs.*, **68**, 189-194 (1946).
7. Martini, W. R., and S. W. Churchill, *A.I.Ch.E. J.*, **6**, 251-257 (1960).
8. Mull, W., and H. Reiher, *Gesund.-Ing. Beihefte*, Reihe 1, No. 28 (1930) (as reported in references 5 and 6).
9. Ostrach, Simon, *Natl. Advisory Comm. Aeronaut. Rept. 1111* (1953).
10. Peaceman, D. W., and H. H. Rachford, Jr., *J. Soc. Ind. Appl. Math.*, **3**, 28-41 (1955).
11. Poots, G., *Quart. J. Mech. Appl. Math.*, **11**, 257-273 (1958).
12. Schmidt, E., and W. Beckmann, *Tech. Mech. Thermodynamik*, **1**, 341-349, 391-406 (1930).
13. Wilkes, J. O., Ph.D. thesis, Univ. Michigan, Ann Arbor (1963).

Manuscript received October 14, 1964; revision received June 18, 1965; paper accepted July 23, 1965. Paper presented at A.I.Ch.E. Boston meeting.